Desalination and Water Treatment
www.deswater.com

doi: 10.5004/dwt.2023.29159

281 (2023) 296–304
January

Evaluation of TiO_2/smectite nanoparticles as an alternative low-cost adsorbent for chromium removal from industrial wastewater

Wala Aloulou[a], Hajer Aloulou[a], Mohamed Romdhani[a], Joelle Duplay[b], Raja Ben Amar[a,*]

[a]*Reserach Unit 'Advanced Technologies for Environment and Smart Cities', Faculty of Science of Sfax, University of Sfax, Tunisia, emails: benamar.raja@yahoo.com (R. Ben Amar), walaaloulou6@gmail.com (W. Aloulou), hajer.aloulou89@yahoo.fr (H. Aloulou), med594268@gmail.com (M. Romdhani)*
[b]*EOST-LHYGES, UMR 7517 CNRS, Université de Strasbourg, France, email: jduplay@unistra.fr*

Received 25 July 2022; Accepted 28 November 2022

ABSTRACT

In this work, chromium removal efficiency from electroplating industry wastewater was studied by adsorption using TiO_2/smectite nanoparticles (NP) synthesized by modification of natural smectite by colloidal route. The effect on chromium adsorption of adsorbent dose, pH, contact time, temperature and initial concentration was then determined in batch system. Chromium concentration can be reduced to 24 mg/L (70%) under the experimental condition (pH = 2.9, adsorbent dose = 1.6 g/L, contact time = 75 min, T = 298 K and C_0 = 80 mg/L) when initial chromium concentration of 80 mg/L is employed. The chromium adsorption on NP was described by the Langmuir isotherm and the maximum chromium adsorption capacity was found as 35 mg/g. Kinetics data were best described by the pseudo-second-order model. The thermodynamic studies proved that the adsorption was exothermic and spontaneous.

Keywords: Adsorption; Chromium; TiO_2/smectite; Nanoparticles; Electroplating industry wastewater; Modeling

1. Introduction

Nowadays, the increased industrialization generates multiple metallic pollutants and causes a serious threat on the environment (air, water and soil) due to the toxicity generated by those substances [1]. Therefore, the treatment of the industrial effluents before their discharge into water bodies is required to minimize the pollution of the water resource [2].

In particular, heavy metals including cobalt (Co), cadmium (Cd), chromium (Cr), lead (Pb) and mercury (Hg), even in trace amounts, cause harmful effects on aquatic fauna such as respiratory irritation and hepatic cell destruction [3–5]. In aquatic environment near industrialized coastline areas, these heavy metals can affect fish, mollusks, tuna [6,7]. Heavy metals are found in wastewater of various industries such as surface treatment time allergy and electroplating industries [8]. Especially, chromium is a toxic contaminant, even in very low concentrations. Chromium in its hexavalent form is the predominant form of chromium species in most water streams and surface water [9]. Cr(VI) is well known for its health-related issues in humans including carcinogenic and mutagenic risks [10,11]. Due to very high solubility and mobility of chromium(VI) ions in ecosystems, chromium(VI) ions are considered the most toxic when compared to other forms of chromium salts [12]. Moreover, Cr(VI) is included in the list of the US Environmental Protection Agency (EPA) as one of the most toxic heavy metals requiring prioritized control. According to the World Health Organization (WHO) standards, the acceptable level of chromium ion in drinking water is 0.05 mg/L for Cr(VI) and 0.1 mg/L for total Cr [13].

The conventional techniques for the removal of chromium(VI) wastes include precipitation, adsorption, membrane processes, oxidation and ion exchange [14,15]. However,

* Corresponding author.

most of these methods results in partial removal of metal ions, low selectivity, high consumption of reagents, high operational cost and production of secondary pollutants [16,17]. Especially, adsorption has distinct advantages which include selectivity for specific metal, reusability of biomaterial, short operation time and low operating cost [18,19].

Bayuo et al. [17] found that the groundnut shell can be an efficient alternative adsorbent material to remove chromium(VI) from aqueous solution. The influence of operating conditions such as contact time, pH, adsorbent dose, initial metal concentrations and temperature was studied. Labied et al. [20] reported that 62.08% of hexavalent chromium removal was achieved by activated carbon obtained from a waste of lignocelluloses material (*Ziziphus jujuba* cores).

In the present work, separation performance of adsorption process during the removal of chromium solution by TiO_2/smectite nanoparticles (NP) was evaluated. The effect of operating parameters such as dose of NP, pH, contact time, temperature and initial concentration on the adsorption capacity of NP during the chromium removal was investigated. Furthermore, adsorption kinetic and isotherm studies were undertaken to determine the adsorbate removal rate and the maximum adsorption capacity. Thermodynamic properties, such as enthalpy, entropy and the free energy were also estimated to provide insight into the adsorption mechanism during the adsorption removal of the chromium. These NP are used in different applications such as membrane separation [15,21–23], hybrid system and adsorption [24] to treat different effluents. High performances of these NP encourage their use in the elimination of heavy metals by adsorption.

2. Experimental procedures

2.1. Materials

The nanoparticles (NP) of TiO_2/smectite were synthesized in a previous work via sol–gel method [18]. The NP powder was obtained by incorporating titanium(IV) isopropoxide with in the organo-modified smectite (Fig. 1). The resulting (NP) have a homogeneous structure with a uniform distribution of the TiO_2 nanoparticles and a mean particle size in the range of 8–12 nm.

2.2. Characterization of NP

The Fourier-transform infrared spectroscopy (FTIR) of purified smectite, cetyltrimethylammonium bromide modified smectite (CTAB/Sm) and NP were obtained by using a PerkinElmer spectrometer to observe the surface functional groups. The zeta-potentials of the samples were determined using a zeta sizer. The measurements were conducted in wide pH range (pH was adjusted with HCl and NaOH aqueous solutions) in order to identify the surface charge of the NP. The average pore sizes, surface areas, and pore volumes of NP were determined using the Brunauer–Emmett–Teller (BET) method and Micromeritics ASAP 2020 apparatus (France).

2.3. Industrial effluent

The industrial wastewater used in this study is produced by a Tunisian electroplating industry. The characterization of the wastewater with initial pH of 2.9 presents chromium concentration of 80 mg/L. Physico-chemical parameters of raw and treated effluents were measured according to the standard methods suggested by American Public Health Association. pH measurement was done by a pH-meter (ISTEK pH-220L, Japan). The content of heavy metals was measured by Atomic Absorption Spectroscopy (AAS) (PerkinElmer AAnalyst 200, France).

2.4. Adsorption in a batch system

Adsorption experiments were performed in batch system. The effect of the operational parameters, adsorbent dosage (0.2–2 g/L), contact time (5–120 min) and temperature (298–303 K) were carried out. All the uptake experiments were conducted using 50 mL of the test solution in 100 mL Erlenmeyer flask on a magnetic shaker at 200 rpm. After equilibrium, the samples were filtered and the filtrate was then analyzed. The percentage of chromium adsorption was calculated as follows by Eq. (1):

$$\text{Adsorption}(\%) = \left(\frac{(C_i - C_f)}{C_i}\right) \times 100 \quad (1)$$

The adsorption capacity of chromium compounds by NP was determined by Eq. (2):

$$q = \left(\frac{(C_i - C_f)}{m}\right) \times V \quad (2)$$

where C_i and C_f are the initial and final (or equilibrium) chromium concentrations, respectively. V is the volume

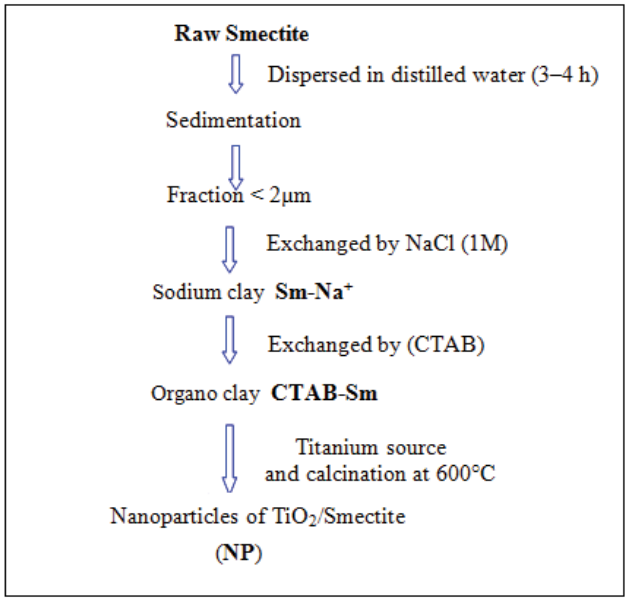

Fig. 1. Preparation of nanoparticles (NP) nanostructured materials based on sol–gel method.

of the chromium solutions (L), and *m* is the weight of the adsorbent (g).

3. Results and discussion

3.1. NP characterization

From our previous work [15,21], the FTIR data shows that the smectite particles are strongly coated with TiO_2 nanoparticles. The point of zero charge (pH_{pzc}) of the synthesized NP was found around 1.7 or 1.8. Therefore, the NP has a negative surface charge in the pH range of 1.7–12. The NP size was determined by BET analysis. The surface area, average pore size and pore volumes of NP were 92 m^2/g, 8–12 nm and 0.19 cm^3/g, respectively. These values are more important than the results of the purified smectite that did not exceed 72 m^2/g [15]. The higher surface area presents more available active sites [25]. As a result, raising the surface area can be a workable tactic for further enhancing adsorption on the NP.

3.2. Adsorption in a batch system

3.2.1. Effect of the NP dose

The effect of the dose of NP on the adsorption of chromium was evaluated by changing the dosage in the range from 0.2 to 2 g/L while the pH and the initial chromium concentration were kept constant at 2.9 and 80 mg/L respectively (Fig. 2). The results showed that the adsorption efficiency increased with the increase of the adsorbent dose. This indicates that the higher the NP dosage, the higher the number of active adsorption sites. However, the removal of the chromium remained unchanged when the adsorbent dose is over 1.6 g/L. This behavior assumes that the adsorption reaction can reach a dynamic equilibrium, and that the maximum chromium removal of 70%, was achieved for a minimum dosage value of 1.6 g/L.

3.2.2. Effect of pH

The performance of Cr(VI) removal is strongly influenced by pH. This parameter is related to the existing of ionic species of Cr(VI) in the solution and also to the surface charge of the adsorbent. The Cr(VI) form shows distinct ionic species. It often takes the forms of $HCrO_4^-$ and $Cr_2O_7^{2-}$ when the pH is between 1 and 6.5. CrO_4^{2-} is the predominant form when the pH is higher than 6.5 (Fig. 3a) [26]. Therefore, the study of the effect of this parameter is very useful to study the mechanism and the interaction adsorbent-Cr(VI). The Cr(VI) adsorption (%) was investigated in the pH range of 2.9–10 as shown in Fig. 3b. The adsorption (%) was strongly decreased from 70% to 12.7% when the pH increased from 2.9 to 10. It is clear that the adsorption was high at low pH (2.9). This behavior can be explained by the electrostatic attractions between the positively charged sites formed under acidic pH condition (H^+ predominate) by the protonation of the NP and the predominate ionic species of Cr(VI) ($HCrO_4^-$) [27]. However, the increasing of the pH caused a reduction in the protonation degree of the NP and consequently the NP ability to interact with Cr(VI) reduced [26,27]. Besides, the –OH in the NP can act as powerful electron donors and it can cause a direct reduction for Cr(VI) to Cr(III). In this, the negative charge surface of the NP can interact with the Cr(III) species and the hydrolyzed form such as $Cr(OH)_2^+$, $Cr_2(OH)_2^{4+}$, and $Cr(OH)_2^+$ [28]. When the pH was over 5, the precipitation of $Cr(OH)_3$ increased as a result of increasing OH^- ions. This precipitation was not uptake by the acidic functional groups of the NP [29]. As a result, the adsorption (%) was

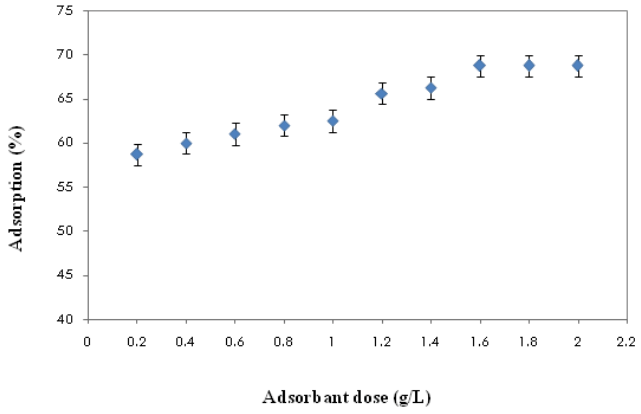

Fig. 2. Effect of adsorbent dose (C_0 = 80 mg/L; V = 50 mL; pH = 2.9; t = 75 min; T = 298 K).

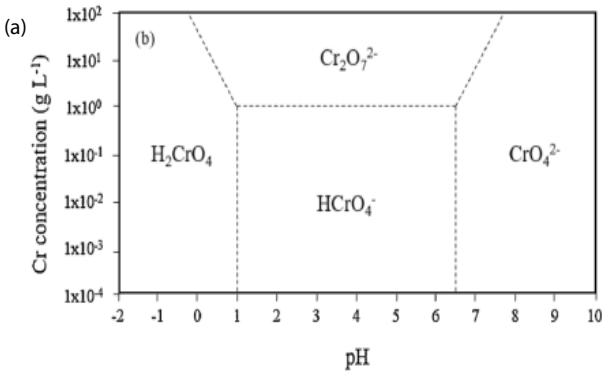

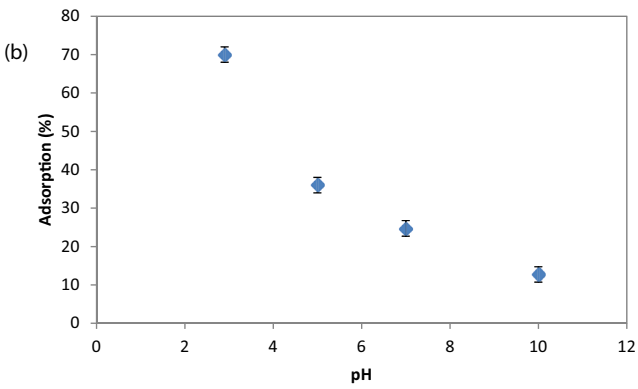

Fig. 3. Distribution of Cr(VI) species in water as a function of pH level and Cr(VI) concentration (a) and effect of pH (C_0 = 80 mg/L; V = 50 mL; t = 75 min; T = 298 K) (b).

strongly reduced at higher pH. Therefore, in this study, the initial industrial wastewater pH of 2.9 was considered for all the experiments.

3.2.3. Effect of contact time

The adsorption efficiency of the chromium onto NP as a function of contact time is illustrated in Fig. 4. It is noticed that the adsorption increases with contact time and reaches equilibrium within 75 min showing a maximum efficiency of chromium retention of about 70%. Therefore, 75 min was selected as the period of optimum contact time for further experiments.

3.2.4. Effect of the temperature

The adsorption of chromium on NP was studied by varying the temperature from 298 to 308 K at the optimal adsorbent dose of 1.6 g/L during 75 min as contact time. According to Fig. 5, chromium removal decreased from 70% to 61% when the temperature increased from 298 to 308 K, leading to a decrease in the adsorption capacity. The increase of the temperature allows the chromium to desorbs from the adsorbent surface to the solution, or to damage the active binding sites in the adsorbent which explains the decrease in the retention of chromium [17]. As a result, the optimum temperature was selected as 298 K for further adsorption experiments.

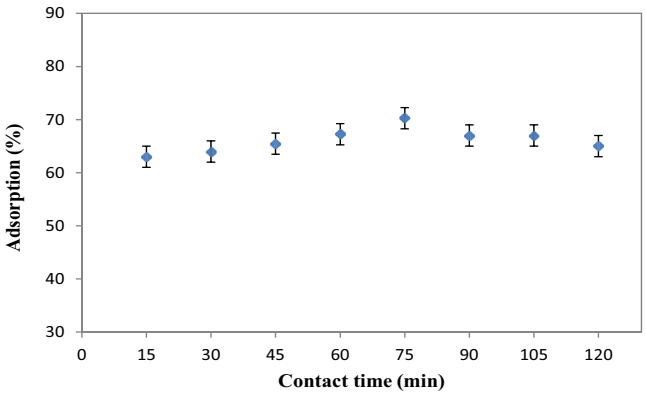

Fig. 4. Effect of contact time (C_0 = 80 mg/L; m = 1.6 g; V = 50 mL; pH = 2.9; T = 298 K).

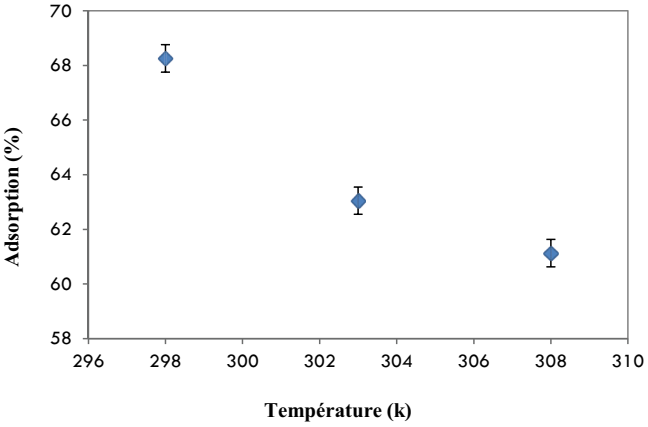

Fig. 5. Effect of temperature (C_0 = 80 mg/L; m = 1.6 g; V = 50 mL; pH = 2.9; t = 75 min).

3.2.5. Effect of initial Cr(VI) concentration

The effect of initial Cr(VI) concentration (20–120 mg/L) on the efficiency of the NP adsorbent was investigated and the adsorption (%) was determined as shown in Fig. 6. The higher efficiency of adsorption (%) of Cr(VI) ions was observed at lower concentrations. Specifically, a total retention was observed for initial concentration between 20 and 40 mg/L. This indicates that for any Cr(VI) solution with a concentration below 40 mg/L, the NP will retain almost totally the Cr(VI) ions. Beyond this value, the adsorption (%) was decreased from 87.3 (at 60 mg/L) to 39 (at 120 mg/L). This behavior might be explained by the large accessible active sites of NP available at low concentration, allowing a total removal of ions [30]. Consequently, 40 mg/L was considered as the highest possible concentration when a dose of NP of 1.6 g/L is used.

3.3. Adsorption kinetics

Adsorption kinetic models are utilized to interpret the experimental data in order to identify the mechanism controlling the adsorption process. The equilibrium data were calculated using kinetic models such as pseudo-first-order, pseudo-second-order and intra particle diffusion model. The pseudo-first-order model can be expressed as follows (Eq. (3) [31]):

$$\ln\left(q_e - q_t\right) = \ln q_e - k_1 t \tag{3}$$

where q_t and q_e are the adsorption capacity (mg/g) at time t (min) and at equilibrium respectively and k_1, the rate constant of the model (min^{-1}). The adsorption rate constants k_1 can be obtained experimentally from the plot of $\ln(q_e - q_t)$ against t (Fig. 7a).

Experimental data were also determined by the pseudo-second-order kinetic model described by Eq. (4):

$$\frac{t}{q_t} = \left(\frac{1}{k_2 q_e^2}\right) + \left(\frac{t}{q_t}\right) \tag{4}$$

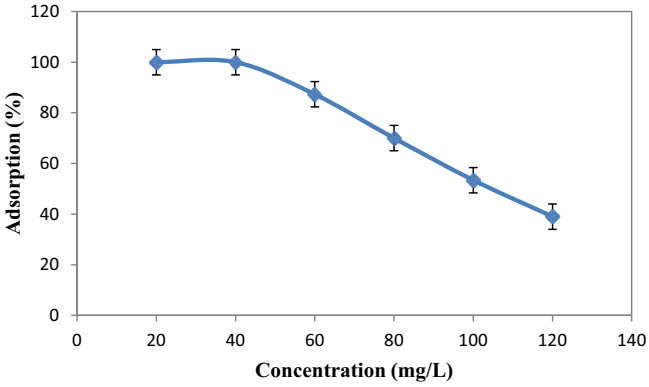

Fig. 6. Effect of initial Cr(VI) concentration (m = 1.6 g; V = 50 mL; pH = 2.9; t = 75 min; T = 298 K).

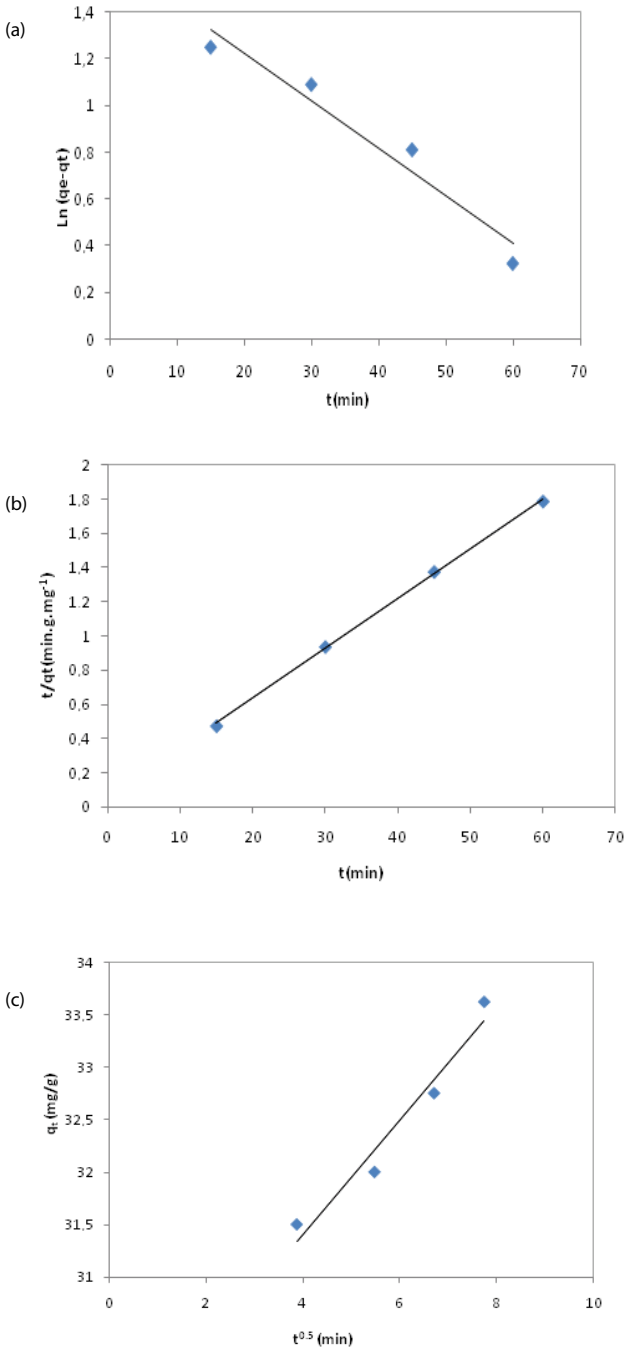

Fig. 7. Pseudo-first-order (a), pseudo-second-order (b) and intraparticle diffusion (c) kinetic plot for the removal of chromium by NP.

where k_2 (g/mg·min) is the rate constant of the model and q_e is the maximum adsorption capacity (mg/g) [32]. The values of k_2 and q_e were determined from the slopes and intercepts of plots of t/q_t against t (Fig. 7b).

The intra particle diffusion model is usually used for identifying the adsorption mechanism for design purposes. The equation related to this model is expressed by Eq. (5) [33]:

$$q_t = k_3 t^{0.5} + C \tag{5}$$

where q_t is the amount of fluoride ion adsorbed (mg/g) at time t (min), k_3 is the intraparticle diffusion rate constant (mg/g·min), which can be calculated from the slope of the linear plots of q_t vs. $t^{0.5}$ and C is the intercept (mg/g) (Fig. 7c).

All constants of the different models are summarized in Table 1. It is clear that the determination coefficient (R^2) obtained from pseudo-second-order model is higher to that found from the pseudo-first-order and intra particle diffusion model. In addition, the value of q_e ($q_{e,\text{cal}}$) determined from the pseudo-second-order model perfectly fitted with the experimental values of q_e ($q_{e,\text{exp}}$), showing that the removal process chromium by adsorption on NP follows the pseudo-second-order kinetic model.

3.4. Adsorption isotherm models

The determination of the adsorption isotherms is important for describing the adsorption mechanism related to the interaction of the chromium ions on the NP adsorbent surface. The determination of the adsorption isotherm corresponds to the distribution of molecules between the liquid phase and the solid phase when the adsorption process reaches an equilibrium state.

In the current work, two sorption isotherm models, Langmuir [34] and Freundlich [35] were studied.

Langmuir model is characterized by the unique coating layer on sorption surface. It can be defined according to the following Eq. (6):

$$\frac{C_e}{q_e} = \frac{1}{\left(q_{\max} K_L\right)} + \frac{C_e}{q_m} \tag{6}$$

The separation factor is expressed by Eq. (7):

$$R_L = \frac{1}{\left(1 + K_L C_0\right)} \tag{7}$$

Table 1
Calculated kinetic parameters for pseudo-first-order, pseudo-second-order and intraparticle diffusion for the removal of chromium by NP

Temperature (K)	$q_{e,\text{exp}}$ (mg/g)	Pseudo-first-order			Pseudo-second-order			Intraparticle diffusion		
		k_1 (min^{-1})	q_e (mg/g)	R^2	k_2 (g/mg·min)	q_e (mg/g)	R^2	k_3 (mg/g·min)	C	R^2
298	35	0.02	3.896	0.945	0.325	34.48	0.999	0.541	29.24	0.953

where q_e the equilibrium chromium concentration on the adsorbent (mg/g), C_e the equilibrium chromium concentration in the solution (mg/L), q_{max} the monolayer adsorption capacity of the adsorbent (mg/g) and K_L the Langmuir adsorption constant (L/mg). The values of Langmuir constants q_{max} and K_L were obtained from the slope and intercept of the linear plot of C_e/q_e against C_e (Fig. 8a). The value of R_L indicates that when R_L is between 0 and 1 the adsorption is favorable, while $R_L > 1$ represents unfavorable adsorption, and $R_L = 1$ represents linear adsorption, while for $R_L = 0$, the procedure of adsorption is irreversible.

The Freundlich isotherm is based on the adsorption on the heterogeneous surface. The linear form of this isotherm can be expressed by Eq. (8) [35]:

$$\log q_e = \log K_F + \left(\frac{1}{n}\right)\log C_e \tag{8}$$

where K_F an empirical constant (mg/g), indicative of the adsorption capacity and $1/n$ an empirical parameter, indicative of the adsorption intensity. The Freundlich isotherm constants K_F and $1/n$ were obtained from the slopes and intercepts of the linear plot of $\log q_e$ vs. $\log C_e$ (Fig. 8b).

Table 2 summarizes the adsorption constants determined according to Langmuir and Freundlich models. It is to notice that the linear equation of Langmuir model presents higher determination constant (R^2 = 0.997) than for the Freundlich model (R^2 = 0.985). Therefore, Langmuir model is chosen as the best model to describe the adsorption of chromium on NP. This model suggests that the retention of chromium implies the coverage of a monolayer on the NP surface.

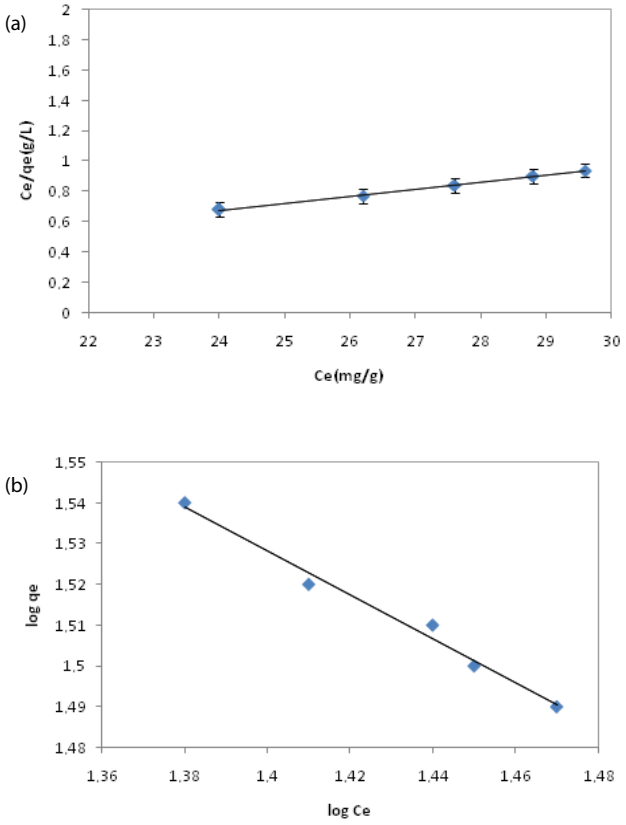

Fig. 8. Isotherm plots for adsorption of chromium onto NP (m = 1.6 g; V = 50 mL; t = 75 min; C_0 = 80 mg/L; T = 298 K: Langmuir (a) and Freundlich (b).

3.5. Adsorption thermodynamics

Temperature is an important parameter affecting the adsorption capacity of sorbents and the transport/kinetic process of the chromium adsorption. Three thermodynamic parameters, including Gibbs free energy change ($\Delta G°$), standard enthalpy change ($\Delta H°$) and standard entropy change ($\Delta S°$) of chromium adsorption on NP were determined by using Eqs. (9) and (10) [36]:

$$\Delta G° = -RT\ln K_d \tag{9}$$

$$\ln K_d = \left(\frac{\Delta S°}{R}\right) - \left(\frac{\Delta H°}{RT}\right) \tag{10}$$

where R is the universal gas constant (8.314 J/mol·K), T is the absolute temperature (K) and K_d is the adsorption equilibrium constant. $\Delta H°$ and $\Delta S°$ values can be determined from the slope and intercept of the Van't Hoff equation by plotting $\ln K_d$ against $1/T$ (Fig. 9). The thermodynamic parameters are summarized in Table 3.

Table 2
Isotherm model parameters for removal of chromium by NP (m = 1.6 g; V = 50 mL; pH = 2.9; t = 75 min; C_0 = 80 mg/L; T = 298 K)

Langmuir		Freundlich	
R^2	0.997	R^2	0.985
q_m (mg/g)	21.73	$1/n$	0.54
K_L (L/mg)	0.103	K_F (mg/g)	192
R_L	0.108	–	–

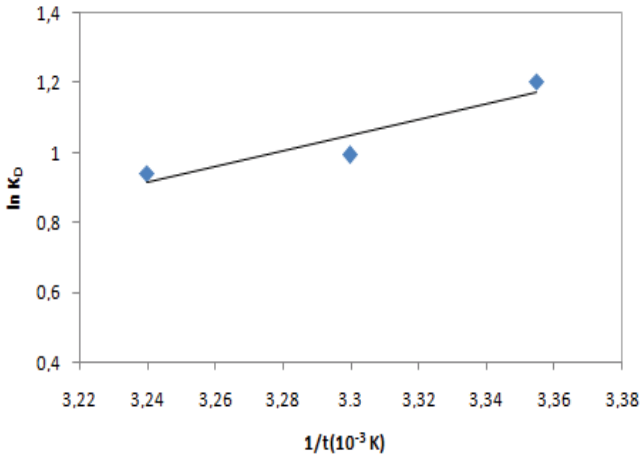

Fig. 9. Plot of $\ln K_d$ vs. $1/T$ for estimation of thermodynamic parameters for adsorption of removal chromium by NP.

The negative values of $\Delta G°$ at different temperatures show the spontaneous nature of the adsorption and the thermodynamically feasible process. The decrease in $\Delta G°$ values with the increase in temperature indicates the possibility of the decrease of the chromium retention at higher temperatures.

The negative $\Delta H°$ (–18.75 kJ/mol) shows that the adsorption process is exothermic. In addition, the adsorption type, physical or chemical, can be determined from the magnitude of enthalpy change. It is conventional that the adsorption is physical when the magnitude of $\Delta H°$ is less than 84 kJ/mol. However chemical adsorption is ranging from 84 to 420 kJ/mol [37]. Therefore, in this study the determination of the $\Delta H°$ value shows a physical adsorption involving weak interaction forces such as van der Waals. The $\Delta S°$ parameter was found to be –53.19 J/mol·K. This negative value suggests reduction in the randomness at the solid/solution interface during the adsorption process [38].

3.6. Adsorption mechanism

In general, the pH affects the degree of ionization and specifications of the adsorbate as well as the surface charge of the adsorbent during adsorption process [17,39]. So the effect of pH directly impacts the electrostatic interactions between the adsorbate and adsorbent's surface.

For the industrial wastewater, at pH 2.9 a large number of H^+ ions exist in the solution medium and the dominant form of Cr(VI) is $HCrO_4^-$. Consequently, the surface protonation of NP leads to the formation of positively charged sites. These protons interact with chromium atoms by an electrostatic attraction phenomenon so that $HCrO_4^-$ is retained on NP [17,20].

Table 3
Thermodynamic parameters for chromium adsorption onto NP

T (K)	$\Delta G°$ (kJ/mol)	$\Delta H°$ (kJ/mol)	$\Delta S°$ (J/mol·K)
298	–2.93		
303	–2.501	–18.75	–53.19
308	–2.409		

4. Discussion

The performances of NP for chromium removal were compared with others nanoparticles reported in the literature (Table 4). Zou et al. [40] synthesized and tested chitosan/attapulgite composites for the removal of Cr(III) from aqueous solution. The maximum adsorption capacity was 65.37 mg/g with adsorbent dosage of 0.2 g/L at pH 5 and a temperature of 45°C. The chromium adsorption was described by Langmuir isotherm and intraparticle diffusion model. Wang et al. [41] prepared chitosan-Al-pillared montmorillonite nanocomposite to remove Cr(VI). They reported that the maximum adsorption capacity of chromium was 15.68 mg/g for pH 6.38 and ambient temperature. On the other hand, the kinetic results indicate that the adsorption of chromium follows the pseudo-second-order model and that the adsorption isotherm is described by the Langmuir model.

Alemu et al. [14] used vesicular basalt volcanic rock to remove Cr(VI). It was reported that the maximum removal achieved at pH 2 was of 79.20 mg/kg at an initial concentration of 5.0 mg/L and adsorbent dosage of 50 g/L. The study of adsorption isotherms shows in this case that the pseudo-second-order kinetic model and the Freundlich isotherm model best describe the adsorption process [14].

Another strategy was developed by Kumar et al. [42] by synthesizing Na-montmorillonite/cellulose nanocomposite as adsorbent. The application of this nanocomposite for the removal of Cr(VI) from industrial wastewater showed an adsorption capacity of chromium of 22.3 mg/g at the pH range 3.8–5.5. The removal kinetics was found to follow the

Table 4
Water treatment for removal Cr(VI) from different inorganic contaminants over clay-polymers nanocomposites (NCs) adsorbents

Adsorbent	Temperature (°C)	pH	Adsorption capacity	Type of solution	Isotherm model	Kinetics model	References
Nanoparticles (NP)	25	2.9	35 (mg/g)	Industrial wastewater	Langmuir	Pseudo-second-order	This study
Chitosan/attapulgite	45	5	65.37 (mg/g)	Aqueous solution	Langmuir	Intraparticle diffusion	[37]
Chitosan-Al-pillared montmorillonite	25	6.38	15.68 (mg/g)	Aqueous solution	Langmuir	Pseudo-second-order	[38]
Na-montmorillonite/cellulose	–	3.8–5.5	22.3 (mg/g)	Aqueous solution	Langmuir	Pseudo-second-order	[39]
Vesicular basalt volcanic rock	25	2	79.20 mg/kg	Aqueous solution	Freundlich	Pseudo-second-order	[14]
Activated carbon	25	2	72.46 mg/L	Aqueous solution	Langmuir	Intraparticle diffusion	[23]
Oxalate modified weak basic resin (IO@D301)	20	5	201.30 mg/L	Aqueous solution	Freundlich	Pseudo-first-order	[24]

pseudo-second-order and the maximum amount adsorbed was best simulated by the Langmuir isotherm model [42].

5. Conclusion

In this work, the potential of NP nanoparticles for the removal of chromium from aqueous solutions was studied. The effect on chromium removal efficiency by NP of the different parameters, such as adsorbent dose, pH, contact time, temperature and initial concentration, was investigated. It was found that the adsorption mechanism followed the Langmuir isotherm model. The monolayer adsorption capacity of NP was of 35 mg/g, adsorbent dose = 1.6 g/L, pH = 2.9, contact time = 75 min, T = 298 K and C_0 = 80 mg/L. The kinetic study of the equilibrium data showed that the removal of chromium ions followed best the pseudo-second-order model. The thermodynamic study indicated the feasibility, exothermic and spontaneous adsorption of chromium onto NP at 298–308 K. Compared to other nanocomposites, NP is a promising material for chromium removal from industrial wastewaters.

Acknowledgments

This paper is supported by the PRIMA program under grant agreement No2024 - TRUST project. The PRIMA program is supported by the European Union. This work was also supported by the Tunisian Ministry of Higher Education and Scientific Research (DGRST) TR in the frame of the SETPROPER research project (grant n°13-043, ERANETMED_WATER program).

Disclosure statement

No potential conflict of interest was reported by the authors. S. Khemakhem, Elaboration and characterization of ceramic microfiltration membranes from natural zeolite: application to the treatment of cuttlefish effluents, Desal. Water Treat., 95 (2017) 9–17.

References

[1] J. Cuhorka, E. Wallace, P. Mikulášek, Removal of micropollutants from water by commercially available nanofiltration membranes, Sci. Total Environ., 720 (2020) 1–11, doi: 10.1016/j.scitotenv.2020.137474.
[2] M.M. Damtie, Y.C. Woo, B. Kim, R.H. Hailemariam, K.D. Park, H.K. Shon, C. Park, J.S. Choi. Removal of fluoride in membrane-based water and wastewater treatment technologies: performance review, Environ. Manage., 251 (2019) 1–24, doi: 10.1016/j.jenvman. 2019.109524.
[3] M. Banni, J. Jebali, M. Daubeze, C. Clerandau, H. Guerbej, J.F.Narbonne, Monitoring pollution in Tunisian coasts: application of a classification scale based on biochemical markers, Biomarkers, 10 (2005) 105–116.
[4] S. Barhoumi, I. Messaoudi, T. Deli, K. Saïd, A. Kerkeni, Cadmium bioaccumulation in three benthic fish species, *Slaria basilisca*, *Zosterisessor ophicephalus*, *Solea vulgaris* collected from the Gulf of Gabes in Tunisia, J. Environ. Sci., 21 (2009) 980–984.
[5] K. Kessabi, A. Kerkani, K. Saïd, I. Messaoudi, Involvement of Cd bioacumulation in spinal deformities occurrence in natural populations of Mediterranean Killifish, Biol. Trace Elem. Res., 128 (2008) 72–81.
[6] H.A. Chaffai, R.P. Cosson, C. Amiard-Triquet, A. El Abed, Physico-chemical froms of storge of metals (Cd, Cu and Zn) and metallothionein-like proteins in gills and liver of marine fish from Tunisia coast: ecotoxicological consequences, Comp. Biochem. Physiol. C: Pharmacol. Toxicol. Endocrinol., 111 (1995) 329–341.
[7] K. Kessabi, A. Navarro, K. Saïd, I. Messaoudi, B. Pifia, Evaluation of environmental impact on natural populations of the Mediterranean Killifish *Aphanius fasciatus* by quantitative RNA biomarkers, Mar. Environ. Res., 70 (2010) 327–333.
[8] T. Panayotova, M. Dimova Todorova, I. Dobrevsky, Purification and reuse of heavy metals containing wastewaters from electroplating plants, Desalination, 206 (2007) 135–140.
[9] M.A. Hashim, S. Mukhopadhyay, J.N. Sahu, B. Sengupta, Remediation technologies for heavy metal contaminated ground water, J. Environ. Manage., 92 (2011) 2355–2388.
[10] J.C. Igwe, A.A. Abia, A bioseparation process for removing heavy metals from waste water using biosorbents, Afr. J. Biotechnol., 12 (2006) 1167–1179.
[11] S.-J. Park, W.-Y. Jung, Removal of chromium by activated carbon fibers plated with copper metal, Carbon Sci., 2 (2001) 15–21.
[12] M. Muthukrishnan, B.K. Guha, Effect of pH on rejection of hexavalent chromium by nanofiltration, Desalination, 219 (2008) 171–178.
[13] M.E. Mahmoud, A.A. Yakout, A.M. Halbas, M.M. Osman, Remediation of Cr(VI) via combined self-redaction and adsorption by chemically modified carbon sorbents, Turk. J. Chem., 40 (2016) 906–920.
[14] A. Alemu, B. Lemma, N. Gabbiye, M. Tadele, M. Teferi, Removal of chromium(VI) from aqueous solution using vesicular basalt: a potential low cost wastewater treatment system, Heliyon, 4 (2018) e00682, doi: 10.1016/j.heliyon.2018.e00682.
[15] W. Aloulou, W. Hamza, H. Aloulou, A. Oun, S. Khemakhem, A. Jada, S. Chakraborty, S. Curcio, R. Ben Amar, Developing of titania-smectite nanocomposites UF membrane over zeolite based ceramic support, Appl. Clay Sci., 155 (2018) 20–29.
[16] D. Wu, C. Niu, D. Li, Y. Bai, Solvent extraction of scandium(III), yttrium(III), lanthanum(III) and gadolinium(III) using Cyanex 302 in heptane from hydrochloric acid solutions, J. Alloys Compd., 374 (2004) 442–446.
[17] J. Bayuo, K. Pelig-Ba Bayetimani, M. Abukari Abdullai, Adsorptive removal of chromium(VI) from aqueous solution unto groundnut shell, Appl. Water Sci., 9 (2019) 107, doi: 10.1007/s13201-019-0987-8.
[18] K. Rahmani, A.H. Mahvi, F. Vaezi, Bioremoval of lead by use of waste activated sludge, Int. J. Environ. Sci. Technol., 3 (2009) 471–476.
[19] B.A. Shah, A.V. Shah, R.R. Singh, Sorption isotherms and kinetics of chromium uptake from wastewater using natural sorbent material, Int. J. Environ. Sci. Technol., 6 (2009) 77–90.
[20] R. Labied, O. Benturki, A.Y. Hamitouche, A. Donnot, Adsorption of hexavalent chromium by activated carbon obtained from a waste lignocellulosic material (*Ziziphus jujuba* cores): kinetic, equilibrium, and thermodynamic study, Adsorpt. Sci. Technol., 36 (2018) 1066–1099.
[21] W. Aloulou, H. Aloulou, M. Khemakhem, J. Duplay, M.O. Daramola, R. Ben Amar, Synthesis and characterization of clay-based ultrafiltration membranes supported on natural zeolite for removal of heavy metals from wastewater, Environ. Technol. Innovation, 18 (2020) 100794, doi: 10.1016/j.eti.2020.100794.
[22] W. Aloulou, H. Aloulou, R. Ben Amar, Clay-based ultrafiltration membranes supTiO_2 and nanocomposite clay materials over zeolite support for oily wastewater purification and heavy metals removal, Desal. Water Treat., 246 (2022) 166–173.
[23] W. Aloulou, H. Aloulou, A. Jadda, S. Chakraborty, R. Ben Amar, Characterization of an asymmetric ultrafiltration membrane prepared from TiO_2-smectite nanocomposites doped with commercial TiO_2 and its application to the treatment of textile wastewater, Euro-Mediterr. J. Environ. Integr., 5 (2020), doi: 10.1007/s41207-020-0145-6.
[24] M. Romdhani, W. Aloulou, H. Aloulou, C. Charcosset, S. Mahouche-Cherguic, R. Ben Amar, Performance studies of indigo dye removal using TiO_2 modified clay and zeolite ultrafiltration membrane hybrid system, Desal. Water Treat., 243 (2021) 262–274.

[25] X.F. Tan, S.S. Zhu, R.P. Wang, Y.D. Chen, P.L. Show, F.F. Zhang, S.H. Ho, Role of biochar surface characteristics in the adsorption of aromatic compounds: pore structure and functional groups, Chin. Chem. Lett., 32 (2021) 2939–2946.
[26] A. Ramirez, R. Ocampo, S. Giraldo, E. Padilla, E. Flórez, N. Acelas, Removal of Cr(VI) from an aqueous solution using an activated carbon obtained from teakwood sawdust: kinetics, equilibrium, and density functional theory calculations, J. Environ. Chem. Eng., 8 (2020) 103702, doi: 10.1016/j.jece.2020.103702.
[27] D. Jia, H. Cai, Y. Duan, J. Xia, J. Guo, Efficient adsorption to hexavalent chromium by iron oxalate modified D301: characterization, performance and mechanisms, Chin. J. Chem. Eng., 33 (2021) 61–69.
[28] J. Liu, X. Wu, Y. Hu, C. Dai, Q. Peng, D. Liang, Effects of Cu(II) on the adsorption behaviors of Cr(III) and Cr(VI) onto kaolin, J. Chem., 2016 (2016) 3069754, doi: 10.1155/2016/3069754.
[29] M.A. Islam, M.J. Angove, D.W. Morton, Recent innovative research on chromium(VI) adsorption mechanism, Environ. Nanotechnol. Monit. Manage., 12 (2019) 100267, doi: 10.1016/j.enmm.2019.100267.
[30] V. Masindi, S. Foteinis, M. Tekere, M.M. Ramakokovhu, Facile synthesis of halloysite-bentonite clay/magnesite nanocomposite and its application for the removal of chromium ions: adsorption and precipitation process, Mater. Today:. Proc., 38 (2021) 1088–1101.
[31] S. Lagergren, Zur Theorie De r Sogenannten, AdsorptionGeloster Stoffe, Kunglia a Sevenska Venten Skapasa Kademiens, Hand Lingar., 24 (1898) 1–39.
[32] YS. Ho, G. Mckay, D.J. Wase, Study of the sorption of divalent metal ions onto peet, Adsorpt. Sci. Technol., 18 (2000) 639–650.
[33] D. Balarak, J. Jaafari, G. Hassani, The use of low cost adsorbent (Canola residues) for the adsorption of methylene blue from aqueous solution: isotherm, kinetic and thermodynamic studies, Colloids Interface Sci. Commun., 7 (2015) 16–19.
[34] I. Langmuir, The adsorption of gases on plane surface of glass, mica, and platinum, J. Am. Chem. Soc., 40 (1918) 1361–1403.
[35] H. Freundlich, Over the adsorption in solution, J. Phys. Chem., 40 (1906) 1361–1368.
[36] L. Wang, J. Zhang, R. Zhao, Adsorption of basic dyes on activated carbon prepared from *Polygonum orientale Linn*: equilibrium, kinetic and thermodynamic studies, Desalination, 254 (2010) 68–74.
[37] E. Errais, J. Duplay, F. Darragi, Efficient anionic dye adsorption on natural untreated clay: kinetic study and thermodynamic parameters, Desalination, 275 (2011) 74–81.
[38] RA. Anayurt, A. Sari, M. Tuzen, Equilibrium, thermodynamic and kinetic studies on biosorption of Pb(II) and Cd(II) from aqueous solution by macro fungus (*Lactarius scrobiculatus*), Chem. Eng. J., 151 (2009) 255–261.
[39] S. Babel, T.A. Kurniawan, Cr(VI) removal from synthetic wastewater using coconut shell charcoal and commercial activated carbon modified with oxidizing agents and/or chitosan, Chemosphere, 54 (2004) 951–967.
[40] X. Zou, J. Pan, H. Ou, X. Wang, W. Guan, C. Li, Y. Yan, Y. Duan, Adsorptive removal of Cr(III) and Fe(III) from aqueous solution by chitosan/attapulgite composites: equilibrium, thermodynamics and kinetics, Chem. Eng. J., 167 (2011) 112–121.
[41] Y.M. Wang, L. Duan, Y. Sun, N. Hu, J.Y. Gao, H. Wang, X.M. Xie, Adsorptive removal of Cr(VI) from aqueous solutions with an effective adsorbent: cross-linked chitosan/montmorillonite nanocomposites in the presence of hydroxy-aluminum oligomericcations, Desal. Water Treat., 57 (2016) 10767–10775.
[42] A.S.K. Kumar, S. Kalidhasan, V. Rajesh, N. Rajesh, Application of cellulose-clay composite biosorbent toward the effective adsorption and removal of chromium from industrial wastewater, Ind. Eng. Chem., 51 (2012) 58–69.